7-1-2013

Visual activity evoked by infrared in humans after dark adaptation

Leslie Olivia Hopkins

L. Olivia Hopkins
Candidate

Biomedical Sciences
Department

This thesis is approved, and it is acceptable in quality and form for publication:

Approved by the Thesis Committee:

Bill Shuttleworth, PhD, Chairperson

L. Donald Partridge, PhD, Mentor

Melissa Gonzales, PhD

Bob Avery, MD, PhD

VISUAL ACTIVITY EVOKED BY INFRARED IN HUMANS AFTER DARK ADAPATION

by

L. OLIVIA HOPKINS

BACHELOR OF SCIENCE
DOCTOR OF MEDICINE
MASTER OF SCIENCE BIOMEDICAL SCIENCES

THESIS

Submitted in Partial Fulfillment of the
Requirements for the Degree of

Master of Science
Biomedical Sciences

The University of New Mexico
Albuquerque, New Mexico

July, 2013

ACKNOWLEDGMENTS

I thank my mentor and friend, Don Partridge PhD. He has spent numerous hours thinking about this project with me and aiding its development. He has encouraged me through the coursework and writing, and is always quick to respond to emails and meeting requests. He has helped me develop ideas and guided me down the correct paths of inquiry. I am encouraged to pursue future endeavors on this topic based on his guidance. He is an excellent role model. Mentoring and teaching come naturally to him. I aspire to implement similar mentoring skills one day in my career.

I thank my dissertation chair, Bill Shuttleworth PhD, for hearing me speak about this idea and encouraging me to research it further. He introducing me to Dr. Partridge and recommended him as my mentor, which I am whole heartedly thankful for. He has given me invaluable guidance through this process, and has been key to my successful completion of this program.

I also thank my committee members, Melissa Gonzales PhD, and Bob Avery, MD, PhD for their valuable recommendations and guidance pertaining to this research and to my professional development. Thanks specifically for discussions about the research design, biostatistical approach, and many other considerations along the way.

I thank the UNM Preventive Medicine Residency Program for their support and protected time to allow me to finish this program in the past two years.

Thank you to QueLab and Bandit for helping me build the equipment necessary to complete this study.

And thank you to my husband, Aryon, for your patience, love and support through this long process.

VISUAL ACTIVITY EVOKED BY INFRARED IN HUMANS

AFTER DARK ADAPTATION

by

L. Olivia Hopkins

B.A., Anthropology, Biology, University of New Mexico, 2003

M.D. Doctor of Medicine, Ben Gurion University of the Negev, 2008

M.S. Biomedical Sciences, University of New Mexico Health Sciences Center, 2013

ABSTRACT

We evaluated the visual response to infrared (IR) in humans after dark adaptation. In seven adult participants, visual perception, visual sensitivity, and the visual response to IR after light adaptation were tested. Over the course of dark adaptation, we found visual perception and sensitivity to our experimental IR stimulus increased, while the relative IR intensity necessary for perception decreased. Visual perception of the IR stimulus was abolished during a transient light exposure; however, when turned back off, perception to the IR stimulus returned for all participants. These novel findings may be relevant for both pre-clinical and clinical visual research.

TABLE OF CONTENTS

LIST OF FIGURES

LIST OF TABLES

Chapter 1

Introduction

Visual impairment is devastating and many of the diseases that cause vision loss have little current treatment and no known cure. Prevention and treatment rely on a thorough understanding of the anatomy and physiology of the visual system. The image-forming pathways associated with visible light have been exhaustively investigated, but the visual response to infrared (IR) is poorly understood. Many clinical modalities use IR to diagnose and treat visual diseases, but pay little attention to potential physiological responses to these wavelengths. The goal of this research is to investigate the visual response to IR in humans with the belief that understanding this process will impact diagnosis and treatment, and provide a description of an alternative form of visual image formation that may benefit those with some forms of visual impairment.

Visual impairment can drastically affect quality of life, especially for those who develop the impairment after infancy. Vision loss can lead to loss of independence by adversely impacting the ability to perform activities of daily living such as driving. Not surprisingly, there is a strong association between vision loss and symptoms of anxiety and depression [1]. The risk of injuries due to falls and fractures is also increased in visually impaired individuals [2].

Visual impairment affects 285 million people worldwide [3]. Of those, 246 million have low vision and 39 million are blind. A predicted rise in prevalence of visual impairment is expected in the U.S. from 3.3 million in 2000 to 5.5 million in 2020

[4]. This will exacerbate the current economic burden of vision loss, which is already $38.2 billion per year in direct and indirect costs [5]. Direct costs are costs associated with the medical treatment of eye diseases including health services, managed care, costs of supplies, labor, equipment, and pharmaceuticals. Indirect costs include lost productivity and earnings of the visually impaired or their caretakers, lost revenue in taxes and spending, impaired quality of life, pain, suffering, rehabilitation, governmental benefit payments, disability modifications needed in the home and for daily activities, and premature death.

The Snellen eye chart uses Snellen fractions that measure acuity of sight by assessing the ability to identify letters or shapes with high contrast at a specific distance [6]. The numerator represents the test distance, 20 feet; while the denominator represents the distance the average eye can see the letters of a certain size on the eye chart. The International Classification of Diseases-10 classifies vision into four levels of function using the Snellen eye chart [7]. 1) Normal vision indicates no impairment with a visual acuity equal to or better than 20/70. 2) Moderate visual impairment includes visual acuity of less than 20/70, but equal to or better than 20/200. 3) Severe visual impairment includes visual acuity of less than 20/200, but equal to or better than 2/400. 4) Blindness indicates visual acuity of less than 20/400 or a corresponding visual field loss of more than 10 degrees in the better eye with the best possible correction. The term ‘low vision’ includes moderate visual impairment and severe visual impairment while the term ‘visual impairment’ includes low vision and blindness.

Approximately 90% of those with visual impairment live in developing countries [3]. The leading causes of visual impairment worldwide are due to uncorrected refractive errors and cataracts [3]. Other causes include glaucoma, age-related macular degeneration, diabetic retinopathy, trachoma, corneal opacities, and a large number of causes that are undetermined [3]. The leading cause of blindness in low and middle income countries is due to cataracts, while in developing or high income countries the leading cause is due to age-related macular degeneration (AMD), a degenerative retinal disease [3]. (The World Bank classifies countries by gross national income (GNI). High income countries have a GNI above US$12,476, and middle income below that number [8].)

The aging population is at increased risk of developing visual impairment, with about 65% of those affected worldwide being age 50 and older [3]. AMD is the leading cause of severe vision loss in individuals over 65 in the US [9]. An estimated 1.75 million people have AMD in the US and another 7.3 million are at risk [9]. Clearly, more people will be at risk for developing age-related visual impairment as the world's population ages.

Another class of degenerative retinal diseases that significantly contribute to visual impairment in all countries and often earlier in life is hereditary retinal dystrophies (HRD) [10]. This term encompasses a large group of genetic diseases such as retinitis pigmentosa, and juvenile forms of macular degeneration, which are further classified into cone-rod dystrophies, corneal dystrophies, Fuch's dystrophy, and Sorsby's macular dystrophy. Retinitis pigmentosa is the most common form of HRD in the second stage of life leading

to blindness through progressive degradation of the rods, followed by the cones, and affecting 1 in 3000 Americans and 1 in 1878 Navajos [11]. Juvenile forms of macular degeneration can affect children, teenagers and adults and are described as dystrophies instead of degenerative diseases in that there is often a loss of function rather than complete degeneration of the photoreceptor cells. The prevalence of juvenile forms of macular dystrophies varies by type and is more rare than retinitis pigmentosa [12, 13]. Importantly, both HRD and AMD are conditions that cause gradual loss of photoreceptor cells or their function, yet the other cellular layers in the retina remain largely intact [14, 15].

The retina lines the back of the eye and is composed of 5 primary structural layers (Figure 1)[16]. The outer nuclear layer, at the most posterior portion of the retina adjacent to the pigment epithelial cells, contains photoreceptor cells called rods and cones. Rods allow for monochromatic vision in low light conditions, called scotopic vision, while cones allow for color vision in brighter light

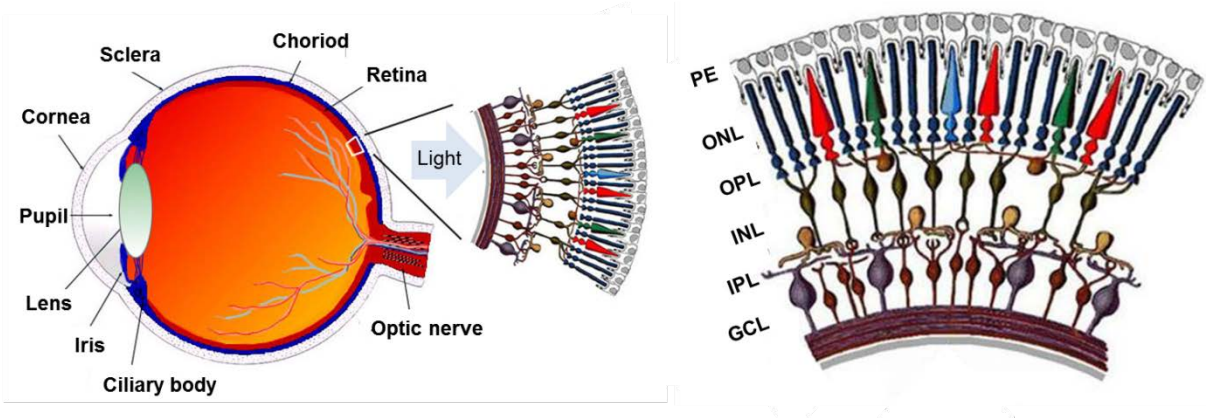

Figure 1. Anatomy of the retina (adapted from Kolb, 1995). A. Cross section through the human eye with a section of retina enlarged. B. Layers of the retina: PE, pigment epithelium; ONL, outer nuclear layer including rods and cones; OPL, outer plexiform layer; INL, inner nuclear layer including bipolar, horizontal, and amacrine cells; IPL, inner plexiform layer; GCL, ganglion cell layer.

conditions, called photopic vision. In the human retina, rods outnumber cones approximately 20:1[17].The next more anterior layer is the inner nuclear layer that includes bipolar, horizontal, and amacrine cells. The most anterior layer, closest to the lens, is the ganglion cell layer. The ganglion cells axons create a nerve fiber layer, which exits the eye as the optic nerve. Neurophil layers divide each of these cell layers, and these are called the outer plexiform layer (OPL) and the inner plexiform layer (IPL) [16]. The photoreceptor cells communicate with the bipolar and horizontal cells through synaptic connections in the OPL, and the bipolar cells communicate with the ganglion cells through synapses in the IPL.

Visual image formation begins when a photon of light enters the eye, passes through the anterior 4 retinal layers, and is absorbed by light-sensitive molecules in a photoreceptor cell. These cells transduce the photon of light into an electrochemical signal, which is communicated to bipolar cells. Rods communicate with ON-bipolar cells, while cones communicate with OFF-bipolar cells. Bipolar cells communicate this signal to ganglion cells where an action potential is generated. These action potentials are propagated via the optic nerve to transmit the signal to the visual areas of the brain, where image perception occurs. The full function of retinal signal processing includes complex interactions through the other retinal interneurons and is much more complex than has been briefly described here.

The visible spectrum of the normal human eye typically ranges from 400 to 700 nm. Photoreceptor sensitivity is dependent on the absorption spectrum of the

photopigments in rods and cones. The retina has four types of photoreceptors including rods, and three types of cones. The photopigment in rods is rhodopsin, while other specialized opsins are found in cones. Cones are classified into short, medium, and long wavelength cones depending on their spectral sensitivities. Each type of cone opsin absorbs a narrow spectrum with a peak and range of wavelengths (Figure 2). The overlapping range of the 3 cone spectra produces a visible spectrum that exhibits differences among testing conditions, individuals, and within an individual's lifetime, with a range reported between 380 – 780nm [18-20].

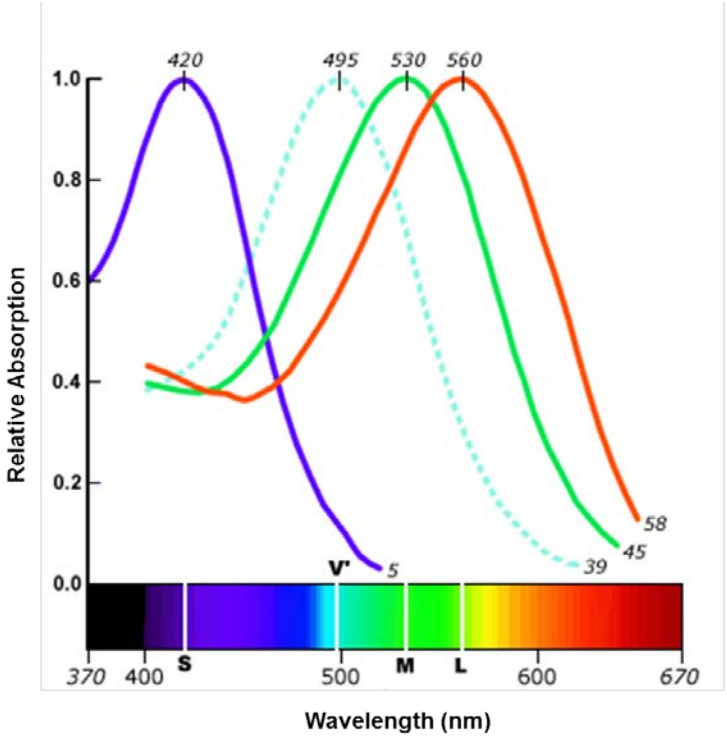

Figure 2. Human photopigment absorption curves (adapted from Dartnall et al, 1983: http://www.handprint.com/HP/WCL/color1.html). Blue = S-cone, Green = M cone, Red = L-Cone, Dashed = Rod)

Age-related macular degeneration causes gradual loss of the photoreceptor cell layer. There are two types of age-related macular degeneration, dry and wet. The dry form occurs when yellow deposits called drusen are deposited in the macula, which is the central portion of the retina where cones are concentrated, causing degradation of image formation [21]. Drusen are composed of acellular, amorphous debris that are deposited between the basement membrane and

retinal pigment epithelium [21]. As the disease advances, the area of drusen deposit grows in size. Initially, there is thinning of the photoreceptor cell layer in the macula, eventually leading to atrophy and cell death. The wet form is characterized by the growth of abnormal blood vessels under the macula, and often occurs after the dry form. These vessels leak fluid into the retina causing distortion of vision. In advanced stages, the macula can scar. The dry form is the most common, accounting for approximately 85 – 90 % of the cases [22].

The most common form of HRD, retinitis pigmentosa, can be caused by a number of different genetic mutations and is characterized by pigment deposits generally leading to the degeneration of rods followed by cones. It is therefore often described as a rod-cone dystrophy [23]. The most common forms of juvenile macular degeneration are cone-rod dystrophies, which are also caused by different genetic mutations. These affect approximately 1/40,000 individuals and are characterized by retinal pigment deposits in the macular region with primary cone loss subsequently followed by loss of rods [13].

Other than trying to slow the progression of AMD and HRD, there is currently no treatment or cure. There are over a dozen groups worldwide that are concentrating on developing vision prosthesis aimed at restoring visual function for patients with these diseases. These prostheses are engineered differently with varying functionalities; however, the premise behind visual prosthesis is to mimic the role of the photoreceptor cells so that information initiated by the prosthesis can directly stimulate the inner nuclear or ganglion cell layers, which remain relatively intact in these degenerative retinal diseases. Prosthesis covert

light to an electrical current either directly through an implanted microchip composed of photodiodes or indirectly through an external source, such as a CCD, attached to an implanted microchip composed of electrodes. Surgical placement of retinal implants varies and includes epi-retinal, sub-retinal, supra-choroidal, trans- scleral, and *ab externo* placement. As of this year, one of these devices became clinically available in in the United States [24], while the others are still under different stages of development.

Prosthesis use silicon-based photodiodes that are responsive to a wide range of wavelengths from 190 to 1100 nm [25]. Infrared (IR) is used to test the prosthesis function by selectively stimulating these devices at the long wavelength end of their sensitivity with the belief that the retina is insensitive to IR. However, retinal sensitivity to IR has been noted during this process [26-29]. These responses were detected in electrophysiologic tests including electroretinography (ERG) and visual evoked potential tests (VEP). ERG measures electrical activity of the retinal cells to a stimulus using an electrode placed on or near the eye. VEP measures the electrical activity of the visual pathway to a light stimulus using electrodes placed on the scalp. The output for both of these tests is an electrical field potential in response to cellular activity in the retina or visual pathway.

Pardue et al evaluated the response of IR in dark adapted cats that had one normal eye and one implanted with a visual prosthesis. They presented evidence, which had been unappreciated in previous studies, that the normal retina had a greater sensitivity to IR on VEP than the implanted eye [26]. Using LEDs with peak emissions at 880nm and 940nm under dark-adapted conditions

a distinct IR-evoked VEP was observed, indicating a visual response in the brain to IR. This response was abolished when a dim light was turned on in the normal eye, but not in the implanted eye.

Concern that the IR response might be a biological response from retinal cells instead of a response from the prosthesis prompted an investigation to determine if retinal cells are sensitive to IR. Gekeler et al. evaluated the retinal response to IR using ERG recording in cats after dark adaptation using both IR LEDs with a peak emission of 875 nm and IR lasers with a peak emission of 826.4 nm (Figure 3) [27, 28]. Lasers, which are monochromatic, were used due to concern that LED output might include emission into the visible spectrum. This study found a scotopic threshold response (STR) that was elicited by both the IR laser and LED in the dark-adapted state, while no discernible ERG response was observed in the light-adapted state. They concluded that the STR was a response from the rod pathway in the dark-adapted state, because the STR ERG response was suppressed once visible light was introduced and the ERG

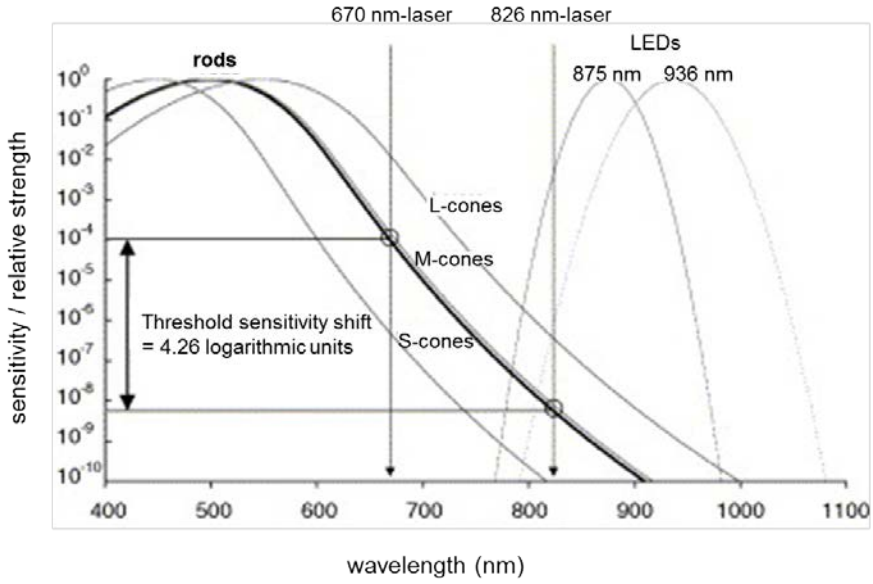

Figure 3. Spectral sensitivity of the cat's photoreceptor pigments (Guenther & Zrenner, 1993) in relation to the spectral distribution of the infrared emitting diodes (IREDs) and the two lasers . (Adapted by Gekeler et al, 2006)

waveforms shifted to the cone pathway. They resolved that IR stimulation of the prosthesis should be done in light-adapted states to prevent the biological response from retinal cells to IR, which they had described in the dark-adapted state.

The STR describes a negative potential in the ERG at threshold under dark-adapted or scotopic conditions in response to very dim light and was first described in 1986 by Sieving et al [30]. They placed microelectrodes at different retinal depths in cats that were dark adapted and then exposed the retina to a very dim light within the visible spectrum. The ERG generated a negative potential near rod threshold and they named this the STR. As light intensity was increased, a b-wave appeared, followed by an a-wave (Figure 4). The a-wave correlates with the response of the rods, while the b-wave correlates with the response of the ON-bipolar cells in the rod pathway. Using aspartate to block synaptic transmission, they found that the STR was generated from processes postsynaptic to the photoreceptors in the rod pathway [31]. Aspartate blocks synaptic transmission from photoreceptors to the bipolar cells at the level of the outer plexiform layer without suppressing the rod or the cone

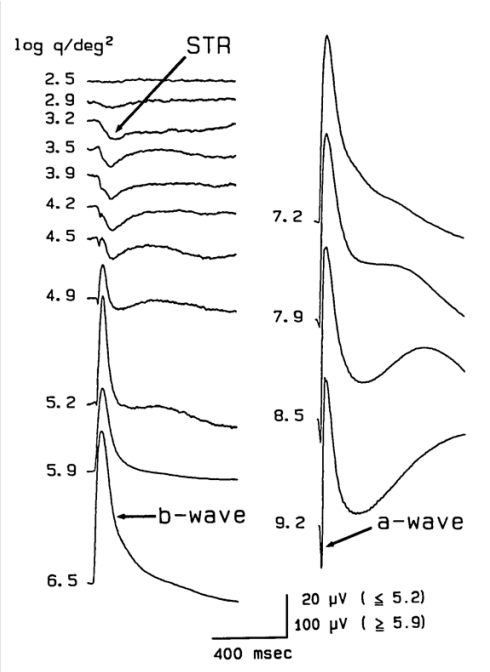

Figure 4. Corneal ERG intensity series of a normal cat using a 10 μsec stimulus (Wakabayashi et al., 1988). The a-wave correlates with a bright stimulus (7.0 – 8.3 log q/deg^2), the b-wave correlates with an intermediate stimuli (3.5 – 6.5), and the STR correlates with dim stimuli (1.6 – 3.6).

response. This results in an ERG with an a-wave with no b-wave [32]. Microelectrode recordings at different retinal levels in cats identified the STR at near the threshold sensitivities of ganglion cells [33]. The STR is now recorded routinely as part of the ERG protocol; however, the exact cell origin of the STR is not known. As described above, IR was also found to elicit a STR in the ERG, which implies that the visual response to IR originates beyond the layer of the photoreceptor layer in the rod pathway.

Other ophthalmic modalities used to diagnosis and treat visual impairment also use IR. Many of these technologies use either Nd:YAG or diode ophthalmic lasers, which emit at 1064nm and 810nm respectively. These ophthalmic instruments include, but are not limited to, optical coherence tomography (OCT) and focal macular electroretinography, both of which use an IR LED fundus camera that can emit IR over a wide range of wavelengths; the confocal laser scanning ophthalmoscope uses an IR light for diagnostic imaging of the eye; indocyanine green angiography uses near IR to assess vascular flow; transpupillary thermal therapy uses IR light from a diode laser to treat intraocular tumors; and infrared autorefractors use IR light to measure the size and shape of the ocular fundus.

Thus, in spite of the common use of IR in ophthalmology, there is indirect, but tantalizing evidence that the visual system may directly respond to IR. Understanding the mechanism by which the visual system responds to IR may benefit both the basic science of vision research and clinical treatments of visual pathologies. First, there are many limiting engineering and biological challenges

to overcome before retinal prosthesis allow for full restoration of sight. Currently, visual prostheses are capable of producing varying degrees of visual acuity from simple perception of light, to simple shapes, and in some cases the resolution necessary to identify letters [34]. A high resolution prosthesis would require thousands of pixels for functional restoration of sight, and these would need to be delivered to the correct retinal cells at an extremely fast rate [35]. As a further complication, progression of retinal degenerative disease leads to reorganization of the layers beyond the photoreceptor cells, and this process is not well understood. Second, there are many clinical modalities that diagnose and treat ocular disease relying on IR. Understanding how the retina responds to IR could improve and advance these technologies. Third, with visual prosthesis to replace lost photoreceptor function, surgery is invasive, and sight restoration of any degree is not guaranteed. However, if a light response could be initiated beyond the photoreceptor layer, manipulating it could potentially allow for vision in diseases lacking photoreceptor cells but with an intact inner nuclear and ganglion cell layers. Finally, with more than 90% of the world's visually impaired living in developing countries, research into alternative ways to improve vision that rely on low cost and high yield mechanisms is especially important.

In this study, we evaluate the visual response to IR after extreme dark adaptation in humans. We believe this IR response may exist in humans based on anecdotal reports of visual perception in conditions that would lead to extended dark adaptation. We hypothesize that: **Infrared (IR) evokes a visual response**

in humans after dark adaptation and that the characteristics of this response suggest transient receptor potential (TRP) channel involvement.

Specifically, we have tested the following three specific aims:

Aim 1: To test if IR elicits a visual response at different time periods of dark adaptation. We hypothesize that IR will elicit an increasing number of correct verbal response as time in the dark increases.

Aim 2: To test if visual sensitivity to IR increases as a function of time. We hypothesize that visual sensitivity to the IR stimulus will increase as the time in the dark increases.

Aim 3: To test if there is a change in IR perception after visible light is reintroduced to the dark adapted eye. We hypothesize the visual response to IR will be abolished after light adaptation.

Chapter 2

Methodology

These experiments were designed to gather information on the feasibility of IR causing a visual response in human participants, since similar studies were done on animals. Three experiments to address the three specific aims were carried out with each participant, all within an hour time frame (Figure 5). Experiment 1 tested if participants could see the stimulus, experiment 2 tested the distance at which participants were able to detect the stimulus, and experiment 3 tested if light adaptation changed the visual perception of the stimulus. In addition, subjective data were collected, which relied on a verbal response of the participant's perception of each experiment.

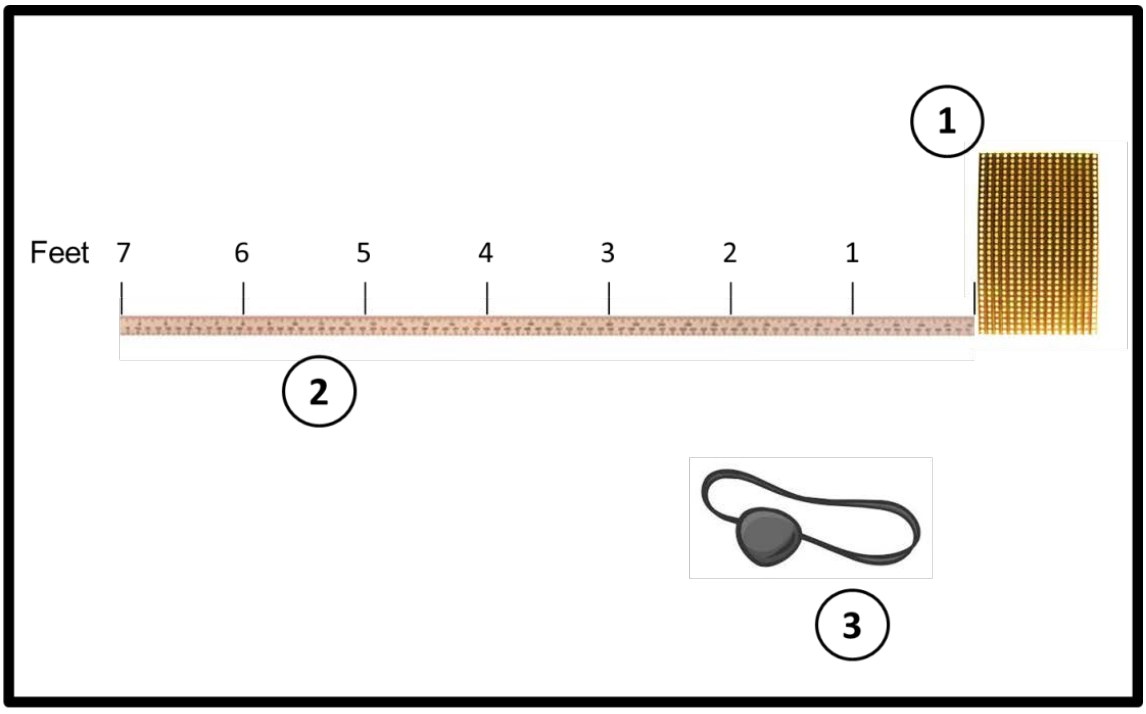

Figure 5. Schematic of the 3 experiments run in the dark room

To our knowledge, the visual perception to IR in humans has not been tested. If one participant has a positive response to all tests in a trial, we consider that trial to be positive and the participant perceived the IR stimulus. In order to demonstrate IR perception in humans is possible, we require at least one trial in this study be correct. Thus, we will assume a low effect size of 10 %, which would produce a 96 % chance of a participant having at least one positive trail, or an 82 % chance that there are two positive trails (Table 1).

Table 1: Power analysis for an effect size of 10 % and 25 % assuming a participant answered all tests in one or two trials correctly. In order for a trail to be considered correct, all tests must be answered correctly

Positive Trial	p = 0.10			p = 0.25		
	n = 15	n = 20	n = 30	n = 15	n = 20	n = 30
≥ 1	0.79	0.88	0.96	> 0.99	> 0.99	> 0.99
≥ 2	0.45	0.61	0.82	0.92	0.98	> 0.99

An infrared light emitting diode (LED) light source was built with a 10 x 10 array of 950 nm LEDs (Panasonic LNA2902L). By the manufacturer's specifications, diodes had a 950nm peak emission wavelength, 50nm (880 -1000nm) spectral half band width and 40° power angle (Figure 6). In our lab, we used a cooled CCD camera (Santa Barbara Instrumentation Group, Model ST10XME) with a spectrometer (SBIG DSS grating spectrometer) to determine the emission spectrum of the diode array in order to critically evaluate the lower wavelength end of the emission spectrum. In a darkroom, we first measured the background ambient light with the spectrometer. The background was 250 counts, which is the background noise of the spectrometer. A count is the measure of the photons

absorbed by a pixel in the CCD and is thus a measure of the image intensity and the spectrometer had a spectral accuracy of less than 1 nm. The exspoure time was 60 seconds total, with the entire CCD array exposed at the same time to the IR LEDs. We found a peak emission at 961nm, which was above the manufacturer's specifications by 11 nm (Figure 7). A second order grating artifact was found at 620 nm and this will be further considered in the Discussion below. The tail or lower end of the emission spectrum rose above background noise to 300 counts starting at 898 nm.

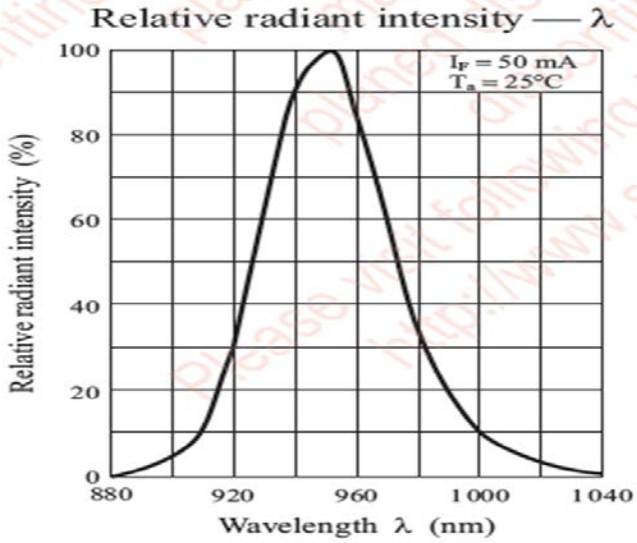

Figure 6. LED Panasonic LNA2902L Specification Sheet. The peak emission is around 950 nm.

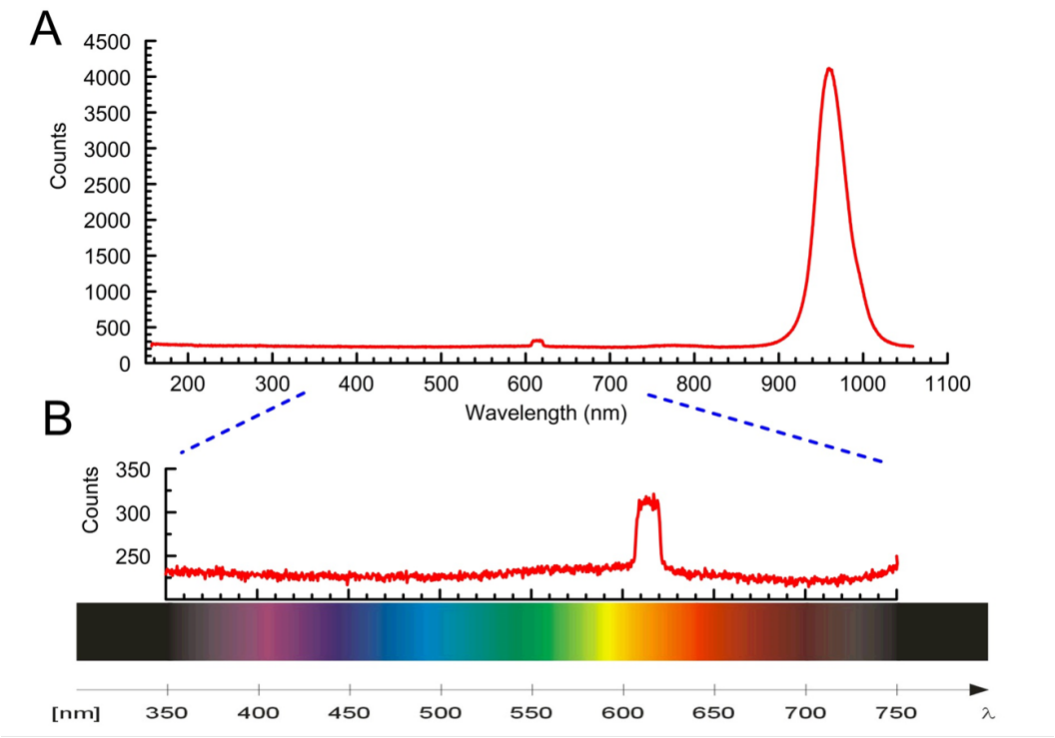

Figure 7. A. Spectral Analysis of IR LED Diode Array
B. Visible Light in the Electromagnetic Spectrum

A light-tight dark room was constructed in the University of New Mexico Clinical and Translational Science Center T1 lab, using a thick black plastic to cover all cracks around the door and a light source from the thermostat. The light in the lab adjacent to this office space was also turned off. The investigator sat in the dark for an hour to allow for dark adaptation of the eyes and then checked for any visible light sources and none were detectable.

The UNM Institutional Review Board (IRB) approved the study through expedited review (HRRC # 12-338). Seven adult participants responded to a volunteer request on a social media website. There was no upper end of age limit; however those under 18 years of age were excluded from the study. There were no other inclusion or exclusion criteria. The study was explained, all questions answered,

and informed consent obtained. Information on general health and visual health were collected by questionnaire. Experiments were carried out individually for each participant in complete darkness as described above.

For Experiment 1, the LED light source was mounted on the wall and participants stood one foot in front of it for each trial of infrared exposure at times 0, 15, 30, 45, and 60 minutes (Table 2). At each time interval, one trial consisted of six tests per individual. A test was defined by the investigator turning on one of two switches; either one that turned on the IR stimulus or dummy one that did not. Participants were instructed to respond to each test with 'yes' if they saw the IR stimulus or 'no' if they did not. A trial consisted of 3 actual and 3 dummy tests delivered in a predetermined order that varied between time intervals and participants All seven participants received one trial at each time interval for a total of 42 tests per time interval. All six tests in a trial had to be answered correctly for the trial to count toward the participant being able to see the stimulus.

Table 2. Number of tests per trail to evaluate, "Can you see the stimulus: Yes or No?"

	0 Minutes	15 Minutes	30 Minutes	45 Minutes	60 Minutes
Participant	**Trial 1**	**Trial 2**	**Trial 3**	**Trial 4**	**Trial 5**
1000	3S/3NS	3S/3NS	3S/3NS	3S/3NS	3S/3NS
1001	3S/3NS	3S/3NS	3S/3NS	3S/3NS	3S/3NS
1002	3S/3NS	3S/3NS	3S/3NS	3S/3NS	3S/3NS
1003	3S/3NS	3S/3NS	3S/3NS	3S/3NS	3S/3NS
1004	3S/3NS	3S/3NS	3S/3NS	3S/3NS	3S/3NS
1005	3S/3NS	3S/3NS	3S/3NS	3S/3NS	3S/3NS
1006	3S/3NS	3S/3NS	3S/3NS	3S/3NS	3S/3NS
n =	42	42	42	42	42

S: Stimulus; NS: No Stimulus

After each trial, participants were asked to describe what they saw while still standing one foot in front of the board while it was on.

Experiment 2 was carried out in an effort to determine the subject's IR sensitivity. Participants were tested at different distances from the light source, the IR stimulus was turned on and the participant gave a verbal response of 'yes' or 'no' if they could see the stimulus, or not. If they replied 'no,' they could not see the stimulus, they were asked to sit down and wait until the next time interval. If they replied 'yes,' they could see the stimulus, they were asked to count the furthest distance back at which they could still see the stimulus. Distance was determined by using a measuring device that was notched with one foot increments and participants backed up counting the notches. Participants reported at how many feet from the IR stimulus they could still it. Experiment 2 followed experiment 1 at each time interval. Relative IR sensitivity was determined by calculating relative intensity of the board at different distances from the inverse square law, intensity $\propto$ 1/distance^2, normalized to the intensity at the board.

The visual angle subtended by the board at each distance was determined for both the height and width of the board from the relationship:

V = 2 arctan (S/2D)

where V is the visual angle, S is the object dimension, and D is the distance from the object (Table 3).

Table 3. Visual angle in degrees at different distances from the IR stimulus.

	1 inch	1 foot	2 feet	3 feet	4 feet	5 feet	6 feet	7 feet
Width	123.73	17.12	8.91	5.95	4.46	3.57	2.98	2.55
Height	111.78	14.03	7.04	4.70	3.52	2.82	2.35	2.01

Experiment 3 was carried out after experiments 1 and 2 were complete. Participants wore an eye patch on one eye and a 3 W 45 lumen LED flashlight LED was shown on the non-patched eye for 30 seconds. Participants looked directly at the light at a distance of approximately 2 feet. The eye with the patch was additionally cupped using one hand to further prevent light leak. After the light was turned off, participants stood one foot in front of the IR stimulus, which was turned on. Participants first reported if there was a difference between the perceived intensity at the final 60 minute trial compared to the perceived intensity after the eye was exposed to light. Next, the eye patch was moved from the dark-adapted eye and used to cover the light-adapted eye, and the comparison was done for the eye that was still dark adapted. Participants then removed the eye patch and reported if they thought there was a difference between the perceived intensity seen by the light- and dark-adapted eyes.

Descriptive statistics were used to quantify demographics and the information obtained from the health questionnaire. IR perception was quantified with a one-sided hypothesis test using binomial proportions to compare proportional differences between the total number of correct responses and the expected number of correct responses (H_o: $x \leq 0.5$; H_I: $x > 0.5$) for each time period. A two-sided Fisher's exact test was used to compare proportional differences between time periods of dark adaptation (H_o: $x = x_1$; H_I: $x \neq x_1$).

A repeated measures logistic regression model was used to account for the within-subject correlation for the dichotomous outcome (correct vs incorrect). We used this design because we collected multiple responses from the same

individuals at different time points. There are a number of assumptions that must be met to apply logistic regression [36]. These include 1) Normality of distribution for each level of the within subject variation, meaning if the null hypothesis is correct, we assume there would be a normal distribution in correct trails at each time period. 2) Sphericity, we assumed the same variance exists between different trials for the within subject factor, and 3) Randomness, the tests for each of our trials were done at random, however the time periods were set, and participants were not chosen at random. 4) Independence of observations, or whether an individual is measured once or several times. We obtained repeated measures by measuring individuals several times, both in each trail, and at each time period. Because our observations were non-independent (several tests on the same individual), we fit a repeated measures logistic regression model to account for the within-subject correlation over time for the dichotomous outcome. Violations to these assumptions can result in a type 1 error [36].

Validity and reliability of the tests at each time interval were found through sensitivity, specificity, and positive or negative predictive values of the participant's response to the stimulus. Sensitivity was defined as the proportion of participants who could see the stimulus and answered correctly when the stimulus was on. Specificity was defined as the proportion of participants who could not see the stimulus and answered correctly that they could not see the stimulus when it was off. A true positive was someone who could see the stimulus and answered correctly that they could see the stimulus. A true negative was someone who could not see the stimulus and answered correctly that they

could not see the stimulus. A false positive was someone who answered they could see the stimulus when in fact it was off. A false negative was someone who answered they could not see the stimulus when it was on. A positive predictive value of the test was the proportion of participants who tested positive, or answered correctly that they could see the stimulus, and could actually see the stimulus. The negative predictive value of the test was the proportion of participants who tested negative or answered that they could not see the stimulus and actually could not see the stimulus.

Participant comments were also described.

Chapter 3

Results

There were seven adult participants in this study aged 26 to 56, five were male, two were female. Five were non-Hispanic white, one was Hispanic, and one was Asian/Pacific Islander. Four used glasses, one wore bifocals, three used contacts and one had normal vision. One had astigmatism, one dry eyes, one had early onset cataracts. None were colorblind. None had a past history of ocular trauma or surgeries.

Experiment 1: To determine visual perception to IR after dark adaptation, participants were exposed to an IR illumination source every 15 minutes and responded to their ability to see the stimulus. The number of correct versus incorrect responses is shown per trial or time period in Table 4.

Table 4. Number of Correct Responses per Trail. Correct and incorrect responses for each participant at each time interval. All 6 tests per trial must be correct for a trial to be counted as the participant perceiving the IR stimulus. C = correct response, I = Incorrect response.

	0 Minutes		15 Minutes		30 Minutes		45 Minutes		60 Minutes	
Participant	**C**	**I**	**C**	**I**	**C**	**I**	**C**	**I**	**C**	**I**
1000	3	3	6	0	6	0	6	0	6	0
1001	3	3	3	3	6	0	6	0	6	0
1002	3	3	3	3	6	0	6	0	6	0
1003	3	3	3	3	4	2	3	3	6	0
1004	3	3	6	0	6	0	6	0	6	0
1005	3	3	6	0	6	0	6	0	6	0
1006	3	3	3	3	6	0	6	0	6	0

C: Correct Response; I:Incorrect Response

Participants 1000, 1004, and 1005 answered all tests correctly starting at 15 minutes and at every time interval thereafter. Thus, they could accurately perceive the experimental IR stimulus with less than 15 minutes of dark adaptation (Figure 8). Six of the participants could perceive the experimental IR stimulus at 30 minutes (Figure 9). The seventh participant, 1003, did not answer all tests correctly until the 60 minute time interval, indicating that this participant could not perceive the experimental IR stimulus until more than 45 minutes of dark adaptation had occurred.

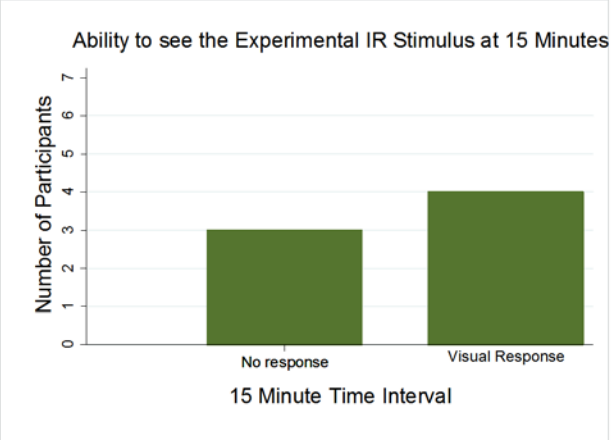

Figure 8. Number of participants able to perceive the experimental IR stimulus at 15 minutes

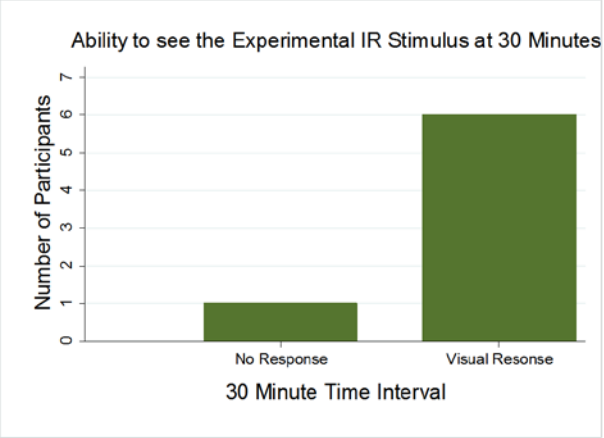

Figure 9. Number of participants able to perceive the experimental IR stimulus at 15 minutes

Proportional differences between the total number of correct responses and the expected number of correct responses were compared for each time period using binomial proportions to quantify IR perception (Table 5). At the initial time point (0

Table 5: Binomial Proportion of Correct Responses

Time (minutes)	Correct Response (%)	Level of significance
0	50.00%	p = 0.5612
15	78.57%	p = 0.0001
30	95.24%	p < 0.0001
45	92.86%	p < 0.0001
60	100.00%	p < 0.0001

minutes) we accept the null hypothesis and participant's responses were no different from chance with correct answers 50% of the time ($p = 0.5612$). At time 15, 30, 45, and 60 minutes, participants answered correctly 79, 95, 93, and 100% of the time ($p \leq 0.0001$), thus we reject the null hypothesis that participants were responding at the chance level. Importantly, at 15 minutes and greater times, the majority of participants were able to see the experimental IR stimulus.

Table 6: Fisher's Exact Test comparing differences in correct answers between time intervals

Time	p value
0 vs 15	$p = 0.012$
0 vs 30	$p < 0.000$
0 vs 45	$p < 0.000$
0 vs 60	$p < 0.000$
15 vs 30	$p = 0.48$
15 vs 45	$p = 0.116$
15 vs 60	$p = 0.002$
30 vs 45	$p = 1.000$
30 vs 60	$p = 0.494$
45 vs 60	$p = 0.241$

We compared the proportion of correct responses between different pairs of time periods. The proportion of correct answers was statistically significant at time zero compared with time intervals 15, 30, 45, and 60 minutes, and between 15 and 60 minutes (Table 6).

Repeated measurements were obtained for each participant at multiple time points, as well as at each time point with multiple responses collected per individual at each trial period. We fit a repeated measures logistic regression model to account for the within-subject correlation over time for the dichotomous outcome (correct vs incorrect). While in this study the within-subject time effect was marginal ($p = 0.0599$). Our results from the hypothesis testing alone may contain a type one error, or an over estimation of the outcomes leading to an incorrect rejection of a true null hypothesis. In future studies with larger sample sizes, fitting a repeated measures logistic regression to the design will the appropriate model to use.

In order to test the validity of the tests at each trial period, statistical sensitivity and specificity were calculated. The specificity of the test, or the proportion of participants who could not see the stimulus and answered correctly that they could not see the stimulus when it was off, was 100% for all trials (Table 7). The sensitivity of the test, or the proportion of participants who could see the stimulus and answered correctly when the stimulus was on, increased as time in the dark increased from 0% at time zero minutes to 100% at 60 minutes. There were no false positives for any of the tests. The number of false negative tests decreased as dark adaptation time increased from 21 tests at 0 minutes to 0 tests at 60 minutes.

Table 7. Validity and Reliability of the Test at Each Time Interval

0 min	**ON**	**OFF**	
Can See Stimulus	(TP) 0	(FP) 0	Sensitivity: 0 % Specificity: 100 % PPV: 0 % NPV: 50 %
Can Not See Stimulus	(FN) 21	(TN) 21	

15 min	**ON**	**OFF**	
Can See Stimulus	9	0	Sensitivity: 42.9 % Specificity: 100 % PPV: 100 % NPV: 65.6%
Can Not See Stimulus	12	21	

30 min	**ON**	**OFF**	
Can See Stimulus	19	0	Sensitivity: 90.5 % Specificity: 100 % PPV: 100 % NPV: 91.3 %
Can Not See Stimulus	2	21	

45 min	**ON**	**OFF**	
Can See Stimulus	18	0	Sensitivity: 85.7 % Specificity: 100 % PPV: 100 % NPV: 87.5 %
Can Not See Stimulus	3	21	

60 min	**ON**	**OFF**	
Can See Stimulus	21	0	Sensitivity: 100 % Specificity: 100 % PPV: 100% NPV: 100%
Can Not See Stimulus	0	21	

PPV: positive predictive value
NPV: negative predicative value

The reliability of the test was determined with the positive and negative predictive values. The positive predictive value, or the proportion of participants who tested positive, by answering correctly that they

could see the stimulus, and could actually see the stimulus, was zero at time zero minutes, and 100% at 15, 30, 45, and 60 minutes. The negative predictive value, or the proportion of participants who tested negative by answering that they could not see the stimulus and actually could not see the stimulus rose from 50 % at the initial time period (0 minutes) to 100 % at 60 minutes.

Table 8. Distance from IR source that stimulus was still visible. "What is the furthest distance in feet you can still see the stimulus."

	0 Minutes	15 Minutes	30 Minutes	45 Minutes	60 Minutes
Participant	**FEET**	**FEET**	**FEET**	**FEET**	**FEET**
1000	----	3	5	6	7
1001	----	----	4	5	6
1002	----	2	3	3	4
1003	----	----	----	----	2
1004	----	6	7	7	7
1005	----	3	3	4	4.5
1006	----	----	3	4	5

FEET: Number of feet from source

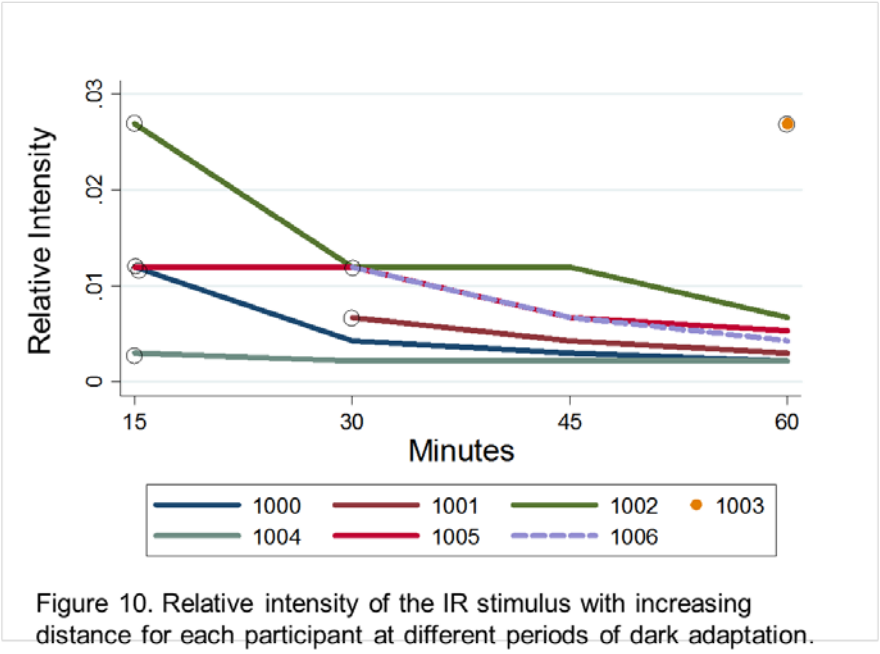

Figure 10. Relative intensity of the IR stimulus with increasing distance for each participant at different periods of dark adaptation. Open circles indicate when the participant first perceived the stimulus.

Sensitivity to the experimental IR stimulus was determining at different distances and at different lengths of dark adaptation (Table 8). At time zero, no one could see the stimulus within one foot of the board. As time elapsed, the ability to see the stimulus from a greater distance increased. The size of the room prevented participants from moving more than 7 feet from the IR stimulus.

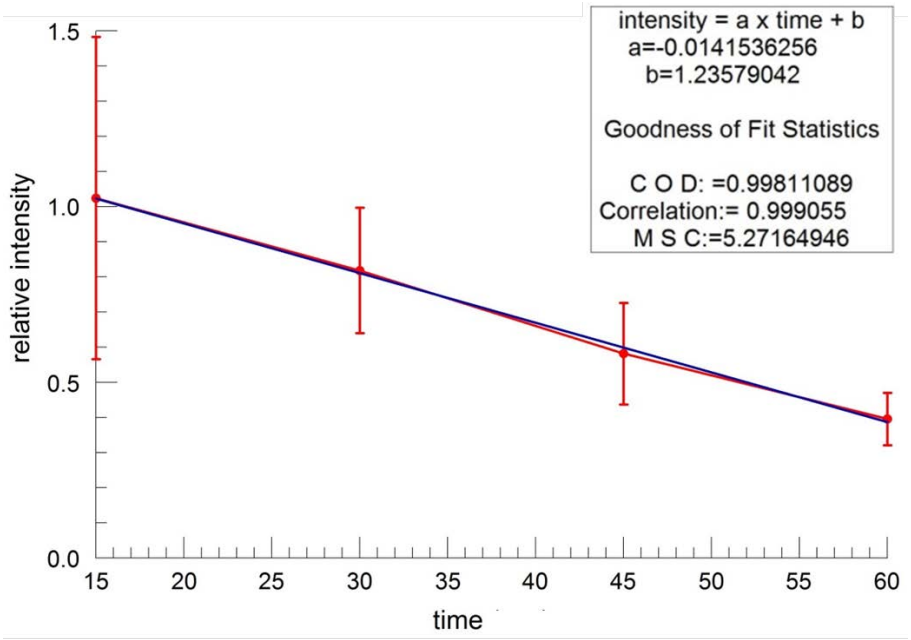

Figure 11. Goodness of Fit test of the average intensity of the experimental IR stimulus over time

The sensitivity to the experimental IR stimulus for each participant was determined by calculating relative intensity of the IR board at different distances based on an inverse square relationship (see Methods) (Figure 10). As time in the dark increased, participants could see lower intensities at further distances from the source.

We assumed participant 1003 to be an outlier. The relative intensities of the IR stimulus at each time period for all of the other participants were averaged

together and fit with a least squares regression (Figure 11). The fit was highly significant for a linear relationship.

After 60 minutes of dark adaptation, participants had one eye briefly light adapted for 30 seconds (Table 9). Four participants reported that the experimental IR stimulus appeared dimmer in the light-adapted eye after light adaptation than before light adaptation, while three reported that it appeared the same, or that there was no difference. All participants reported that there was no difference in perception of the experimental IR stimulus for the dark-adapted eye. The four that perceived a dimmer response of the light-adapted eye also reported that the stimulus was perceived to be dimmer in the light-adapted eye than in the dark-adapted eye.

Table 9. Eye Patch Experiment.

Participant	Dark Adapted (DA) Eye	Light Adapted (LA)Eye	Comparison Both eyes
1000	Same	Same	No difference
1001	Same	Same	No difference
1002	Same	Same	No difference
1003	Same	Dimmer	Dimmer in LA
1004	Same	Same	No difference
1005	Same	Dimmer	Dimmer in LA
1006	Same	Dimmer	Dimmer in LA

Chapter 4

Discussion

Summary of methods

We evaluated the visual response to IR in humans after dark adaptation. In a dark environment, participants were exposed to series of illumination tests from an experimental IR LED source at 15 minute increments of dark adaptation to test visual perception. Sensitivity to IR was determining by calculating the relative IR intensity perceived at different distances and at different time periods of dark adaptation. Finally, visual perception to the experimental IR source was determined after a brief reintroduction to bright light.

Summary of results

At time zero, responses were consistent with the null hypothesis that participants were guessing if the experimental IR stimulus was on or not. As time progressed, responses became consistent with rejecting the null hypothesis and we concluded that participants were able to see the experimental IR stimulus. The sensitivity and negative predictive values of the test increased with time in the dark to 100% at 60 minutes. The specificity of the test was 100% at all time intervals. Positive predictive value was 100% for all time intervals other than time zero, where it was 0%.

Participants were asked to determine at what distance they could still see the experimental IR stimulus. At time zero, no one could see the stimulus at any

distance. As dark adaptation time increased, the ability to see the experimental stimulus increased at progressively greater distances, which was equivalent to viewing the stimulus at lower relative IR intensities.

Participants had one eye briefly exposed to a bright light. Immediately after light exposure, they were all able to perceive the experimental IR stimulus with the light-exposed eye as they had at 60 minutes of dark adaptation. When the light was on, the IR stimulus was not visible to any of the participants.

Discussion of results

Visual sensitivity to the experimental IR stimulus increased in proportion to the length of dark adaptation that the participants experienced. When testing visual perception of the experimental IR stimulus using a series of actual and dummy stimulus presentations at different time intervals, we expected a 50% correct response rate if participants were guessing. We observed this at time zero. As the duration of dark adaptation increased, there was a statistically significant increase in correct responses of participants to the stimulus we used. Furthermore there was a significant increase in correct responses at all time intervals compared to responses at time zero. At the 45 min interval, every response of all but one participant was correct. After one hour, everyone could see the stimulus and 100% of responses were correct, indicating that one hour of dark adaptation consistently unmasks sensitivity to the IR stimulus we used in the eye.

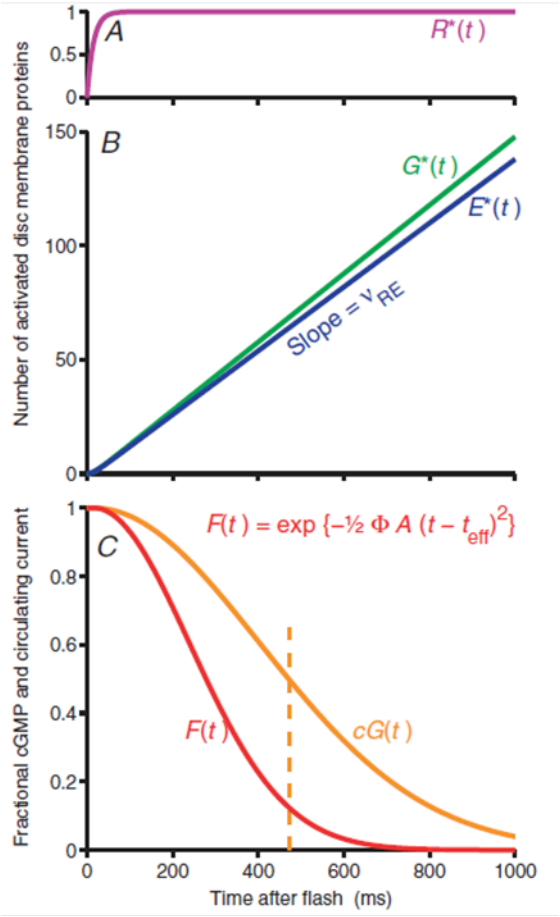

Figure 12 . Predicted time course of the amphibian rod's electrical response (Lamb and Pugh, 2006). (A) Single Rod activation after photoisomerization. (B) Rod activation byproducts: activated G-protien and PDE increase linearly. (C) Flash delivering a flux = 100 photoisomerizations

Phototransduction in rods occurs with the absorption of a photon by the photopigment rhodopsin causing a rapid conformational change in the protein. Within milliseconds, the photopigment 'bleaches' or loses its visible color (Figure 12) [17]. Rhodopsin concentrations are dependent on the coupling efficiency of the rhodopsin G-protein-coupled receptor's ability to transform from inactive to active, and may be less than 100% [17]. Rhodopsin begins to regenerate once it is no longer exposed to light, as the result of a process called dark adaptation, during which visual sensitivity to dim light recovers. It generally takes longer than 15 minutes for 100% of rhodopsin regeneration to occur in a normal retina (Figure 13) [17]. Four of our participants could see the stimulus at 15 minutes, an additional two at 30 minutes and the final participant at 60 minutes. If IR sensitivity is dependent on 100 % of rhodopsin regeneration, we would not have expected correct responses at 15 minutes; however, dark adaptation can vary

among individuals, and be greatly delayed with some types of ocular diseases [17].

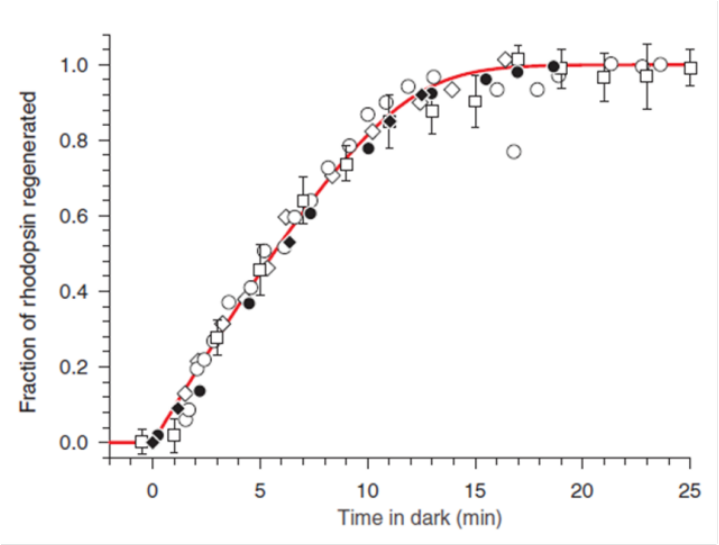

Figure 13. Regeneration of rhodopsin in the human retina (Lamb and Pugh, 2006).

To evaluate whether light exposure abolished the visual sensitivity to the experimental IR stimulus we used, a bright light was introduced to one eye for 30 seconds while participants wore an eye patch over the other to keep it dark adapted. We anticipated that photoreceptor bleaching would eliminate IR sensitivity. However, every participant reported still being able to see the experimental stimulus in the light-exposed eye. In a similar experiment to evaluate the recovery time of rhodopsin in the human retina after exposure flashes of light, Pugh exposed normal human subjects to 30 seconds of visible light at nine different intensities in order to bleach 5 % to 98 % of rhodopsin (Figure 14) [37]. By plotting the log threshold elevation as a function of time in the dark, he found that the dark adapted recovery time has several phases depending on the intensity of the light exposure. For high intensity exposures

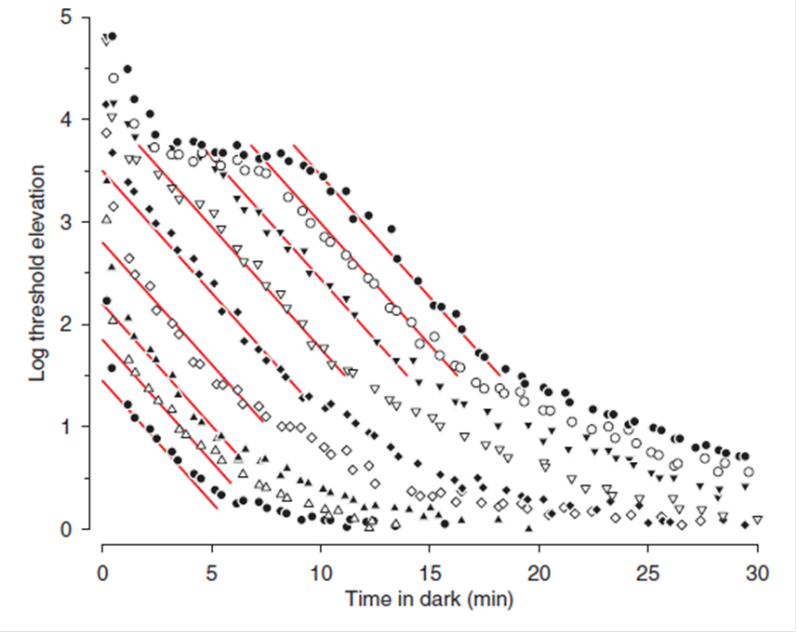

Figure 14. Human psychological dark adaptation (Lamb and Pugh, 2006). Recovery of rhodopsin is plotted as a function of time after a range of bleaching exposures of 30 seconds Moving left to right, bleaching of rhodopsin was estimated at 0.5%; 2%; 4%; 8%; 22%; 39%; 63%; 86%; and 98%. The red line indicates the S2 phase.

there was a cone-mediated recovery, a cone plateau, and finally a rod-mediated recovery. Lower intensity exposures resulted in a rod-mediated recovery only. After about 10 minutes, the rod-mediated recovery became more sensitive than the cone-mediated recovery. The rod-mediated recovery was additionally split into two phases. First, the 'S2' region, indicated by the straight lines in Figure 14 represents the exponential decay of a threshold-elevating substance produced in the bleaching process [17]. The second region reflects the declining level of this substance as it continues to recover. However, even under low intensity exposure, there was still a recovery time of greater than 5 minutes. Our participants did not have sufficient time to begin to undergo dark adaptation again since they looked at the IR source immediately after the bright light was turned off. The intensity of the light used for the 30 second flash was approximately 45 lumens.

It is unclear why the IR response was preserved. One intriguing possibility is that the visual response to IR is not directly generated in the photoreceptor cells, but results from a mechanism occurring elsewhere in the retina. However it is important to note that IR sensitivity to our stimulus was not observed until a minimum of 15 minutes of dark adaptation, suggesting that the rod pathway is somehow involved. As described above, IR produced a STR in the ERG of cats after dark adaptation [28] that was localized to the rod pathway, but originating postsynaptic to the photoreceptor cell layer [30]. Saszid et al found the STR to originate in the inner retina proximal to the bipolar cells [38]. They suggest that the STR is an amacrine or ganglion cell response, and demonstrate that it is extremely sensitive, since it is desensitized by background illuminations that were too weak to elicit a b-wave or an a-wave response, or a response from the rods or bipolar cells.

The known visible spectrum is reported to range from 380 nm to 780 nm in humans. Although visual sensitivity to IR has been reported in cats, rats, and rabbits, to our knowledge, this is the first report that humans have visual perception to IR under dark adapted conditions. We found a visual sensitivity to IR from a LED source with a peak intensity at 950nm. This wavelength falls outside of the known spectral sensitivities of human photopigments for rods, S-cones, M-cones, or L-cones.

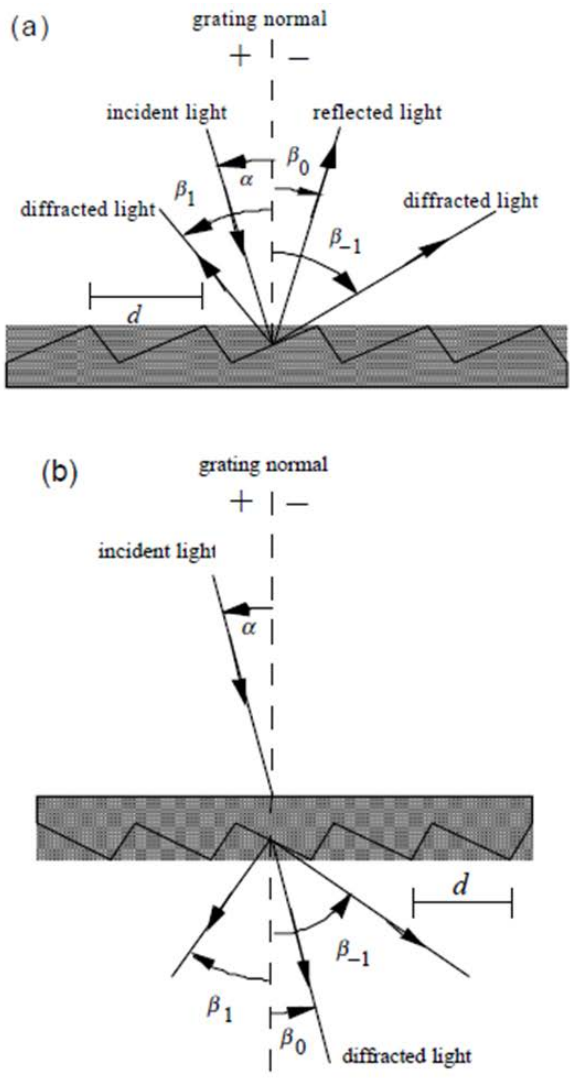

Figure 15. Diffraction grating of a monochromatic light (Palmer, 2005) with incidence land diffraction light rays.
A. Reflection grating: both incident and diffractive rays are on the same side.
B. Transmission grating: incident light and diffractive rays are on opposite sides of the reflective surface

To control for the possibility that the lower end or tail of the emission spectrum of the IR LEDs fell in the visible spectrum, we used a cooled CCD spectrometer to determine the LED spectral emission over a broader range than was provided by the manufacturer's specifications.(see Methods for details). A second order grating artifact was found at 620 with the low resolution lens of the spectrometer. Diffraction gratings are a reflective surface etched with fine lines that produces spectral separation because the angle of diffracted light is different for different wavelengths of incident light. In CCD spectrometers, the intensity of the diffracted light is measured as a function of the diffraction angle. Grating artifacts can occur as a result of imperfections in the reflective surface, such as uneven spacing in the microetched grooves and can appear as misplaced spectral lines (Figure 15) [39]. To complicate things,

overlapping diffraction grating reflections can occur leading to higher order spectral reflections (Figure 16) [39]. These do not represent actual emission wavelengths of the source, but rather predictable higher order diffraction lines. We evaluated the IR source using low, medium, and high resolution lenses in the spectrometer and found that the intensity of the two observed artifacts decreased with the medium and high resolutions lenses. Had they been source emission peaks, we would have expected the intensity to increase with the medium and high resolution lenses. In addition, had there been an actual 620nm emission peak, we would expect participants to perceive a yellow-orangish color, which no one described. Finally, the emission curve is a Gaussian curve, while the grating artifact is a square curve. Had the artifact been real, we would expect it to also be a Gaussian curve.

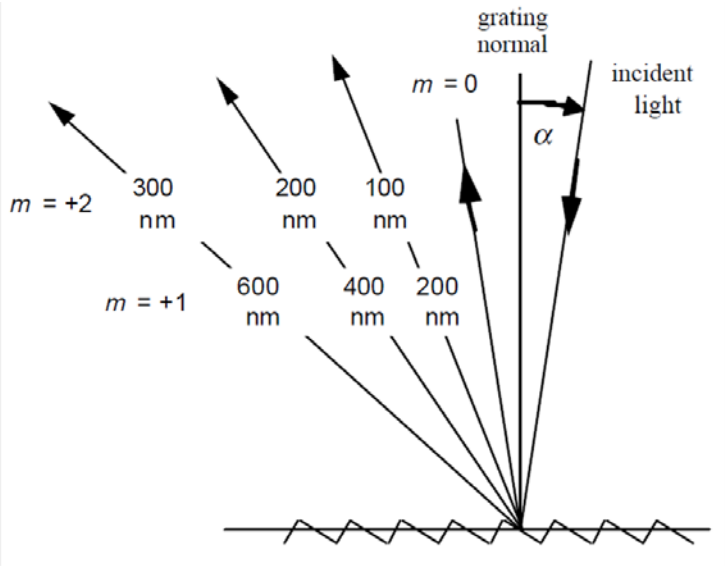

Figure 16. Overlapping of spectral orders (Palmer, 2005). The first order wavelengths of 200 400 and 600 diffract in the same direction as the second order wavelengths of 100, 200, and 300nm.

A potential explanation for the IR sensitivity that we observed in the participants in this study might be explained by examining the mechanism of IR perception in other animals. There are four vertebrate families that detect IR through specialized sensory organs; these include pit vipers, boas, pythons, and vampire bats. In 2010, Gracheva et al. found that all three families of snakes detect IR with transient receptor potential ankyrin 1 (TRPA1) channels located on sensory nerve fibers of the trigeminal nerve that innervates pit organs [40]. Prior to this, the mechanism to IR detection was unknown and there was debate as to whether IR detection in snakes was a photochemical or thermoreceptive process. Transcriptome profiling found a 400 fold increase of TRPA1 in the trigeminal ganglia of the western diamondback rattlesnake (*Crotalus atrox*) compared to the dorsal root ganglia, which provides somatosensory input to the trunk. The rattlesnakes, which have much greater IR acuity than pythons and boas, also had much higher concentrations of TRPA1 channels in the trigeminal ganglion than did the other two families of snakes. No opsin-like sequences, as would be expected in photoreceptors, were found in either ganglion from any of the snakes. Together, these findings indicate that TRPA1 is responsible for IR detection in these snakes, and that the process is through thermosensation. TRPA1 channels are not heat sensitive in other vertebrates, but rather activated by allyl isothiocyanate (AITC), a compound in wasabi and mustard plants. In snakes, they were found to also be sensitive to AITC. At room temperature they were insensitive; however, they became very active at a temperature threshold of 28.0 +/- 2.5 C.

The following year, Gracheva et al found that transient receptor potential vanilloid 1 (TRPV1) channels located on trigeminal nerve fibers, which innervate the ‘leaf pits,’ were responsible for IR detection in vampire bats [41]. TRPV1 is a known heat sensitive channel that detects noxious heat in somatic afferents in vertebrates. Gracheva et al found that TRPV1 gene splicing determined the thermal activation threshold. If the gene was spliced short (TRPV1-S), the thermal threshold of activation was 30.5 +/- 0.7 C, in contrast to the long splice (TRPV1-L), which had a threshold of 39.6 +/- 0.4 C. Splicing of TRPV1-S occurs exclusively in the trigeminal ganglia and not in the dorsal root ganglia, preserving the function of TRPV1 as a detector of noxious heat in somatic afferents. The short and long forms were both present in the trigeminal ganglion. When both forms were present, an intermediate temperature activation threshold occurred at 33.9 +/- 1.2 C, rather than a biphasic threshold, suggesting the formation of heterotetrameric complexes. Interestingly, TRPA1 channels were insensitive to heat in bats.

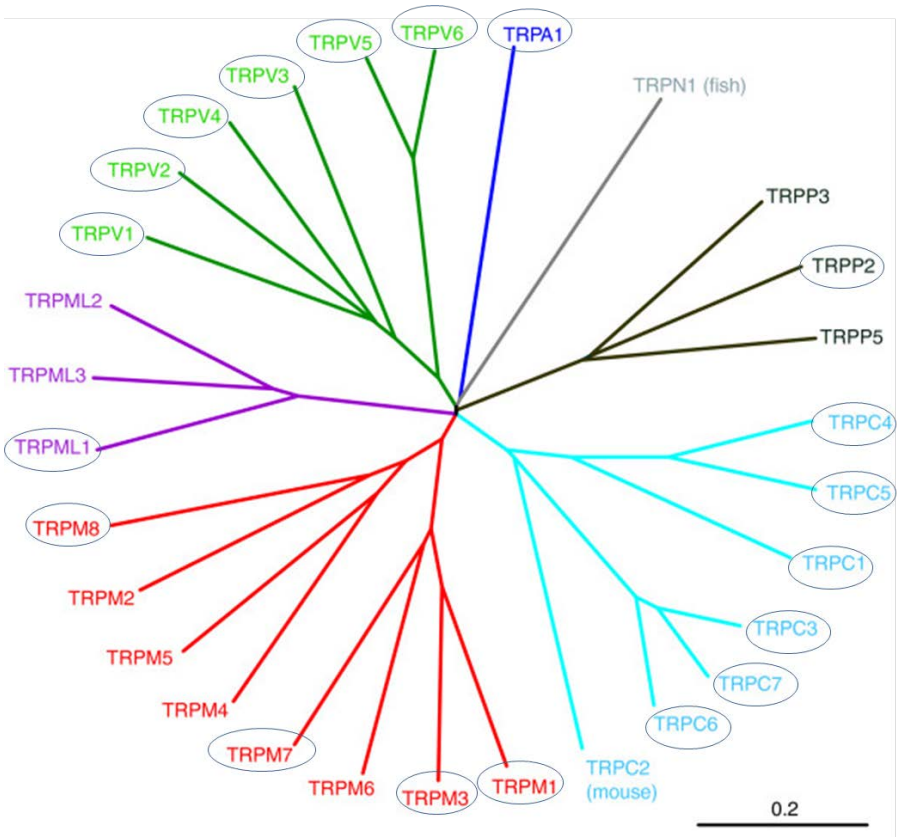

Figure 17. Phylogenetic tree of TRP channels in mammals (adapted from Nilius, 2011). Circles indicate TRP channels reportedly found in the eye of a human or mouse. TRPC2 was not included because humans do not possess this gene.

Transient receptor potential (TRP) channels are cation channels that were first discovered in photoreceptors of *Drosophilia melanogaster* in 1977 [42, 43]. This superfamily can be classified into seven subfamilies, of which six occur in humans; altogether they are encoded by a total 27 different TRP genes (Figure 17) [44]. Since their discovery, research on TRP channels has grown dramatically. They are found in virtually every organ system and cell type [44] that has been investigated including our central and peripheral sensory systems where they are involved in vision, taste, olfaction, hearing, touch, thermosensation, and thermoregulation, as well as homeostatic functions and motile functions in muscles and vessels. As a superfamily, TRP channels are

unique because they are activated and modulated by a wide range of stimuli, which varies between and within subfamilies. Yet, their complete mechanism of activation is still unknown.

Table 10. TRP channels in the mammalian eye by location

Receptor	Location
TRPM1	ON Bipolar Cells (h,m), melanopsin-expressing photosensitive retinal ganglion cells (pRGCs), ciliary body (m), and inner nuclear layer (m)
TRPM3	Muller cells (m), ciliary body (m), outer plexiform and inner nuclear layer (m), retinal pigmented epithelium (m)
TRPM7	cone outer segment (m)
TRPM8	corneal nerve (h)
TRPA1	corneal nerve (h)
TRPP2	cone outer segment (m), multiple layers (m)
TRPML1	outer plexiform and nuclear layer (m), multiple layers (m),
TRPC1	Photoreceptor inner segment layer (m), multiple layers (m), corneal epithelium (h)
TRPC3	ipRGCs (m), multiple layers (m), corneal epithelium (h)
TRPC4	multiple layers (m), corneal epithelium (h)
TRPC5	INL cells adjacent to the inner plexiform layer (m),
TRPC6	ipRGCs (m), RGC (m), corneal epithelium (h)
TRPC7	ipRGCs (m), corneal epithelium (h)
TRPV1	RGCs (m), RPE (h), microglial (m), blood vessels (m), astrocytes (m), synaptic boutons of both retinal plexiform layers (m), cell bodies of the inner nuclear layer (m), ganglion cell layer (m), higher expression in peripheral than central retina, corneal epithelium (h), corneal endothelium (h), corneal nerve (h), ophthalmic branch of the trigeminal nerve
TRPV2	RGCs (m), RPE (h), Photoreceptor axons in the outer plexiform layer (m), retinal plexiform layer(m), cellular bodies in the inner nuclear layer (m), ganglion cell layer (m), corneal epithelium (h), corneal endothelium (h)
TRPV3	RGCs (m), RPE (h), corneal epithelium (h), corneal endothelium (h)
TRPV4	RGCs (m), Dendrites of Retinal Ganglion Cells (RGCs) (m), Muller glial cells, RPE(h), inner plexiform layers (m), cell cytosol and neurites or RGCs (m), corneal epithelium (h), corneal endothelium (h)
TRPV5	RPE (h)
TRPV6	RPE (h)

h: human; m: mouse; ipRGC: intrinsically photoreceptor rental ganglion cells; RPE: retinal pigment epithelial cells

All six subtypes of TRP channels are present in the human and mouse eye. Specific visual involvement is outlined in Table 10, which describes where the channel has been found and which species it was found in [45, 46]. The TRPV 1 to TRPV4 channels are of similar phylogenetic origins, and are selective for calcium and magnesium. They are known heat sensitive channels, with sensitivities to different temperatures. TRPV1 is activated at 43° C, TRPV2 at 52°

C, TRPV3 at 33° C, and TRPV4 below 33° C [47, 48]. All four are found in retinal ganglion cells. It is plausible that any one if not all of the TRPV 1 to TRPV4 channels are responsible for visual sensitivity to IR under dark adapted conditions, based on their sensitivity to heat and the STR sensitivity to IR located at the level of the ganglion cell layer. This could also explain why the STR is so sensitive to increasing illumination. As the photoreceptor cells respond to light, the ganglion cells are activated to transmit the signal to the brain. This photic response may override the responsiveness of the ganglion cells to IR. However, it is still unclear why we observed a consistent response persisting after a brief reintroduction to light.

Based on observations reported in the literature, we hypothesize that IR bypasses the photoreceptive cells and stimulates a visual response through TRP channels elsewhere in retina, one possibility being the TRPV channels in the retinal ganglion cells. The rod pathway is most likely involved in this process, due to the 15 to 30 minute delay that we observed in IR sensitivity and due to the reported presence of an IR sensitive STR after dark adaptation, which is associated with the rod pathway. However, once dark adaptation has occurred, the response seems to become independent of the rods themselves, as evident in ERGs consisting of only a STR and no a-wave or b-wave, and the finding that the response persists after a brief light adaptation of the rods.

There are several clinical implications of these findings. First, to our understanding, other than ERG there are no set parameters for testing the visual response to IR after dark adaptation in any of the standard diagnostic

ophthalmologic instruments. There is a need to further describe this process through these modalities. Furthermore, it should be determined if current ophthalmologic measurements are affected by this response to IR and if so to what degree. The scope of utility for these devices may change or broaden based on this information.

Second, our hypothesized pathway for IR perception could provide an opportunity to restore vision in patients with retinal degenerative diseases with intact ganglion cell layers. One possibility is to create a dark adapted environment through the use of tight fitting goggles that contained a filter selective for a range of IR wavelengths. Of course, vision in this instance would be restricted to sources in the IR wavelength range. The relative intensity on our IR board was high; however the intensity needed to see the stimulus decreased as dark adaptation increased. It is not clear if it would be necessary to amplify the IR intensity in a normal setting for visual perception to occur with such goggles. Another related option is to convert a visible image to IR that could then be directly transduced by TRP channels in the retina. This could be done using a CCD camera to transmit pixels to an LCD display in the goggles. The LCD changes the transmission of light from a backlight source, in this case the backlight source would be IR LEDs adjusted to the best IR reception of the retina. This has the potential to take advantage of a naturally occurring process of IR perception without the need for the retinal implant surgery used in current prostheses.

There are a number of other possibilities to explore for the visual perception to IR. First, when two long wavelength photons are absorbed simultaneously by a photosensitive molecule, the absorption is equivalent to that of a single photon at a shorter wavelength; this is called two-photon absorption (TPA) [49]. The two photons can be of the same wavelength or different wavelengths and the energy change is from a lower state to a higher state. This means that two photons of IR could be absorbed by a photopigment and perceived as visible light. While this is a possibility, it is unlikely that normal incident IR would produce TPA in retinal rhodopsin. Second, a phosphene is the experience of perceiving a light, when there is actually no light entering the eye [50]. These phenomena are thought to result in a normal visual system due to non-photic stimuli. Phosphenes can be induced by magnetic, mechanical, and electrical stimulation of either the retina or visual cortex and are perceived as flashes of light. If the phenomenon that we observed were the result of phosphenes, we would expect participants to describe flashes of light rather than describing the IR LED board in detail. Third, intrinsically photosensitive retinal ganglion cells (ipRGC) are melanopsin-containing ganglion cells that are photosensitive to wavelengths between those of S-cones and rods, in the blue-green range with a peak absorption of 480nm [51]. They contribute to non-image-forming functions including the circadian rhythm, pupillary light reflex, and sleep regulation [52]. While they may also contribute to some aspects of vision, their absorption wavelength is inconsistent with IR sensitivity.

Limitations of the Study

There were a number of limitations of this introductory study. The low sample size could introduce statistical bias. The appropriate statistical tests were run to try to prevent this bias, and a larger sample size will be important for future studies. Outcomes were based on participant's verbal response. Future studies should be designed to use electrophysiologic diagnostic tests to measure visual responses and to correlate these with the verbal response. As mentioned above, the requirement of participants moving to the IR source may have introduced errors. Future studies should be designed so that the IR source will be moved toward a seated subject.

Implications for Future Direction

We hypothesize that TRP channels are responsible for human perception of IR in the dark-adapted eye. The next steps of this research will be to evaluate the electrophysiologic response to IR and to evaluate retinal diseases that eliminate IR sensitivity. This would provide clues as to the nature of TRP channel involvement in the process. It would also be important to evaluate the range of IR spectrum sensitivity of humans and to determine the receptors and pathway involved in the process.

Conclusions

We evaluated the visual response to IR in humans after dark adaptation by testing the visual perception and visual sensitivity to the experimental IR stimulus. Then we evaluated if light adaptation abolished this response. As the

time of dark adaptation increased, visual perception increased to 100% of participants. Visual sensitivity also increased. Light adaptation abolished the response when the light was on. However, if turned off, visual perception to the stimulus was still possible.

The known visible spectrum is between 380 nm to 780 nm. Although visual sensitivity to IR has been reported in cats, rats, and rabbits, to our knowledge, this is the first report that humans have visual perception to IR under dark adapted conditions. We found a visual sensitivity to our experimental IR LED source with a peak intensity at 960nm. We believe this response might occur in the rod pathway via the TRPV channels in ganglion cells; however, more information is needed. This may have clinical implications in both vision research and in diagnosing and treating visual pathologies

I became interested in this topic more than ten years ago, after hearing anecdotal reports from spelunkers describing what seemed like visual perception to IR after extreme dark adaptation. I felt at that time that manipulation of this visual response could have broader implications in the field of vision research.

References

1. Kempen, G.I. and G.A. Zijlstra, *Clinically Relevant Symptoms of Anxiety and Depression in Low-Vision Community-Living Older Adults.* Am J Geriatr Psychiatry, 2013.

2. Wood, J.M., et al., *Risk of falls, injurious falls, and other injuries resulting from visual impairment among older adults with age-related macular degeneration.* Invest Ophthalmol Vis Sci, 2011. **52**(8): p. 5088-92.

3. Organization, W.H. *Global Data On Visual Impairments, 2010*. 2012.

4. Pascolini, D. and S.P. Mariotti, *Global estimates of visual impairment: 2010.* Br J Ophthalmol, 2012. **96**(5): p. 614-8.

5. Wittenborn, J.S., et al., *The Economic Burden of Vision Loss and Eye Disorders among the United States Population Younger than 40 Years.* Ophthalmology, 2013.

6. Kniestedt, C. and R.L. Stamper, *Visual acuity and its measurement.* Ophthalmol Clin North Am, 2003. **16**(2): p. 155-70, v.

7. Deafness, W.H.O.P.o.B.a., *ICD Update and Revision Platform: Change of Definition of Blindness*, in *ICD-10: International Statistical Classification of Diseases and Related Health Problems. Tenth Revision*2004, World Health Organization: Geneva.

8. Bank, T.W., *Data. Country Classification*, in *World Bank Atlas*2013, The World Bank Group.

9. Friedman, D.S., et al., *Prevalence of age-related macular degeneration in the United States.* Arch Ophthalmol, 2004. **122**(4): p. 564-72.

10. Gilbert, C. and A. Foster, *Childhood blindness in the context of VISION 2020--the right to sight.* Bull World Health Organ, 2001. **79**(3): p. 227-32.

11. Heckenlively, J., et al., *Retinitis pigmentosa in the Navajo.* Metab Pediatr Ophthalmol, 1981. **5**(3-4): p. 201-6.

12. Shah, M., et al., *Causes of visual impairment in children with low vision.* J Coll Physicians Surg Pak, 2011. **21**(2): p. 88-92.

13. Hamel, C.P., *Cone rod dystrophies.* Orphanet J Rare Dis, 2007. **2**: p. 7.

14. Santos, A., et al., *Preservation of the inner retina in retinitis pigmentosa. A morphometric analysis.* Arch Ophthalmol, 1997. **115**(4): p. 511-5.

15. Jones, B.W. and R.E. Marc, *Retinal remodeling during retinal degeneration.* Exp Eye Res, 2005. **81**(2): p. 123-37.

16. Kolb, H., *Simple Anatomy of the Retina*, in *Webvision: The Organization of the Retina and Visual System*, H. Kolb, E. Fernandez, and R. Nelson, Editors. 1995: Salt Lake City (UT).

17. Lamb, T.D. and E.N. Pugh, Jr., *Phototransduction, dark adaptation, and rhodopsin regeneration the proctor lecture.* Invest Ophthalmol Vis Sci, 2006. **47**(12): p. 5137-52.

18. Stockman, A., L.T. Sharpe, and C. Fach, *The spectral sensitivity of the human short-wavelength sensitive cones derived from thresholds and color matches.* Vision Res, 1999. **39**(17): p. 2901-27.

19. Curtis, B., *Invitation to Biology: Fifth Edition*1994, New York: Worth Publishers.

20. Lapedes, D., *Dictionary of Scientific & Technical Terms: Second Edition* 1978, New York McGraw Hill.

21. Abdelsalam, A., L. Del Priore, and M.A. Zarbin, *Drusen in age-related macular degeneration: pathogenesis, natural course, and laser photocoagulation-induced regression.* Surv Ophthalmol, 1999. **44**(1): p. 1-29.

22. Wong, T.Y., et al., *The natural history and prognosis of neovascular age-related macular degeneration: a systematic review of the literature and meta-analysis.* Ophthalmology, 2008. **115**(1): p. 116-26.

23. Hamel, C., *Retinitis pigmentosa.* Orphanet J Rare Dis, 2006. **1**: p. 40.

24. Administration, U.F.a.D. *FDA News Release*. FDA approves first retinal implant for adults with rare genetic eye disease 2013 [cited 2013 May 13]; Available from: http://www.fda.gov/NewsEvents/Newsroom/PressAnnouncements/ucm339824.htm.

25. Held, G., *Introduction to Light Emitting Diode Technology and Applications, Chapter 5*, 2008, Auerbach Pub.

26. Pardue, M.T., et al., *Visual evoked potentials to infrared stimulation in normal cats and rats.* Doc Ophthalmol, 2001. **103**(2): p. 155-62.

27. Gekeler FE, S.K., Blatsios G, Zrenner K, *Infrared Irradiation produces scotopic threshold responses (STRs) after prolonged dark-adaptation in cats.* ARVO Meeting Abstract, 2004. **45**(E-abstract): p. 4204

28. Gekeler, F., et al., *Scotopic threshold responses to infrared irradiation in cats.* Vision Res, 2006. **46**(3): p. 357-64.

29. Chow, A.Y., et al., *Implantation of silicon chip microphotodiode arrays into the cat subretinal space.* IEEE Trans Neural Syst Rehabil Eng, 2001. **9**(1): p. 86-95.

30. Sieving, P.A., L.J. Frishman, and R.H. Steinberg, *Scotopic threshold response of proximal retina in cat.* J Neurophysiol, 1986. **56**(4): p. 1049-61.

31. Wakabayashi, K., J. Gieser, and P.A. Sieving, *Aspartate separation of the scotopic threshold response (STR) from the photoreceptor a-wave of the cat and monkey ERG.* Invest Ophthalmol Vis Sci, 1988. **29**(11): p. 1615-22.

32. Levinger, E., E. Zemel, and I. Perlman, *The effects of excitatory amino acids and their transporters on function and structure of the distal retina in albino rabbits.* Doc Ophthalmol, 2012.

33. Frishman, L.J. and R.H. Steinberg, *Intraretinal analysis of the threshold dark-adapted ERG of cat retina.* J Neurophysiol, 1989. **61**(6): p. 1221-32.

34. da Cruz, L., et al., *The Argus II epiretinal prosthesis system allows letter and word reading and long-term function in patients with profound vision loss.* Br J Ophthalmol, 2013. **97**(5): p. 632-6.

35. Winter, J.O., S.F. Cogan, and J.F. Rizzo, 3rd, *Retinal prostheses: current challenges and future outlook.* J Biomater Sci Polym Ed, 2007. **18**(8): p. 1031-55.

36. DSSC, *Repeated Measures ANOVA Using SAS PROC GLM*, in *SPSS*, D.o.S.a.S. Computiona, Editor 1997, The University of Texas at Austin: Austin TX.

37. Pugh, E.N., *Rushton's paradox: rod dark adaptation after flash photolysis.* J Physiol, 1975. **248**(2): p. 413-31.

38. Saszik, S.M., J.G. Robson, and L.J. Frishman, *The scotopic threshold response of the dark-adapted electroretinogram of the mouse.* J Physiol, 2002. **543**(Pt 3): p. 899-916.

39. Palmer, C., *Chapter 2, The Physics of Diffraction Gratings*, in *Diffraction Grating Handbook, 6th ed*, E. Loewen, Editor 2005, Newport Corportation: Rochester, NY.

40. Gracheva, E.O., et al., *Molecular basis of infrared detection by snakes.* Nature, 2010. **464**(7291): p. 1006-11.

41. Gracheva, E.O., et al., *Ganglion-specific splicing of TRPV1 underlies infrared sensation in vampire bats.* Nature, 2011. **476**(7358): p. 88-91.

42. Minke, B., *The History of the Drosophila TRP Channel: The Birth of a New Channel Superfamily.* Journal of Neurogenetics, 2010. **24**(4): p. 216-233.

43. Minke, B., *Drosophila mutant with a transducer defect.* Biophys Struct Mech, 1977. **3**(1): p. 59-64.

44. Nilius, B. and G. Owsianik, *The transient receptor potential family of ion channels.* Genome Biol, 2011. **12**(3): p. 218.

45. Zan Pan, J.E.C.-A.a.P.S.R., *Advances in Ophthalmology*, in *Transient Receptor Potential (TRP) Channels in the Eye*, M. Shimon Rumelt, Editor 2012, InTech: Rijeka, Croatia.

46. Gilliam, J.C. and T.G. Wensel, *TRP channel gene expression in the mouse retina.* Vision Res, 2011. **51**(23-24): p. 2440-52.

47. White, J.P., L. Urban, and I. Nagy, *TRPV1 function in health and disease.* Curr Pharm Biotechnol, 2011. **12**(1): p. 130-44.

48. Numazaki, M. and M. Tominaga, *Nociception and TRP Channels.* Curr Drug Targets CNS Neurol Disord, 2004. **3**(6): p. 479-85.

49. Terenziani, F.K., C; Badaeva, E; Tretiak, S; Blanchard-Desce, M, *Enhanced Two-Photon Absorption of Organic Chromophores: Theoretical and Experimental Assessments.* Advanced Materials, 2008. **20**: p. 2641-4678.

50. Chen, S.C., et al., *Simulating prosthetic vision: I. Visual models of phosphenes.* Vision Res, 2009. **49**(12): p. 1493-506.

51. Hatori, M. and S. Panda, *The emerging roles of melanopsin in behavioral adaptation to light.* Trends Mol Med, 2010. **16**(10): p. 435-46.

52. Pickard, G.E. and P.J. Sollars, *Intrinsically photosensitive retinal ganglion cells.* Rev Physiol Biochem Pharmacol, 2012. **162**: p. 59-90.